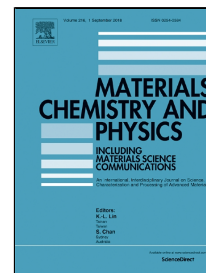


## Accepted Manuscript

Texture evolution and plastic anisotropy of commercial purity titanium/SiC composite processed by accumulative roll bonding and subsequent annealing



Mohsen Karimi, Mohammad Reza Toroghinejad, Hamed Asgari, Jerzy A. Szipunar

PII: S0254-0584(18)30692-8  
DOI: 10.1016/j.matchemphys.2018.08.027  
Reference: MAC 20870  
To appear in: *Materials Chemistry and Physics*  
Received Date: 23 March 2018  
Accepted Date: 10 August 2018

Please cite this article as: Mohsen Karimi, Mohammad Reza Toroghinejad, Hamed Asgari, Jerzy A. Szipunar, Texture evolution and plastic anisotropy of commercial purity titanium/SiC composite processed by accumulative roll bonding and subsequent annealing, *Materials Chemistry and Physics* (2018), doi: 10.1016/j.matchemphys.2018.08.027

This is a PDF file of an unedited manuscript that has been accepted for publication. As a service to our customers we are providing this early version of the manuscript. The manuscript will undergo copyediting, typesetting, and review of the resulting proof before it is published in its final form. Please note that during the production process errors may be discovered which could affect the content, and all legal disclaimers that apply to the journal pertain.

# Texture evolution and plastic anisotropy of commercial purity titanium/SiC composite processed by accumulative roll bonding and subsequent annealing

Mohsen Karimi<sup>a, 1</sup>, Mohammad Reza Toroghinejad<sup>b</sup>, Hamed Asgari<sup>c,d</sup>, Jerzy A. Szpunar<sup>d</sup>

<sup>a</sup> Faculty of Chemical and Materials Engineering, Shahrood University of Technology, Shahrood 3619995161, Iran

<sup>b</sup> Department of Materials Engineering, Isfahan University of Technology, Isfahan 84156–83111, Iran

<sup>c</sup> Department of Mechanical and Mechatronics Engineering, University of Waterloo, Waterloo, ON, Canada

<sup>d</sup> Department of Mechanical Engineering, University of Saskatchewan, Saskatoon, SK S7N 5A9, Canada

## Abstract

In this study, commercial purity titanium (CP–Ti) with SiC particle reinforcements produced using accumulative roll bonding (ARB) process and subsequent annealing. Texture evolution and plastic anisotropy in different steps of the process were studied. ARBed material exhibited a significant magnitude of anisotropy of mechanical properties. Moreover, a strong TD split basal texture with basal poles tilted 25° away from the normal direction toward the transverse direction was developed in the ARBed samples. Higher normal anisotropy obtained for ARB–annealed sheet, compared to that of the starting titanium sheet, indicated lower susceptibility to thinning. However, ARB–annealed sheet exhibited higher planar anisotropy ( $\langle\Delta r\rangle=0.048$  for ARB–annealed sheet and  $\langle\Delta r\rangle=-0.434$  for starting titanium). Higher resistance to thinning of the ARB–annealed sheets compared to the starting titanium was ascribed to the higher uniform elongation shown by annealed sheets. Furthermore, it was concluded that finer grain size of ARB–annealed sheet resulted in higher work hardening of the sheet, which in turn, increased the uniform elongation of ARB–annealed sample.

**Keywords:** Accumulative roll bonding; Titanium; Texture; Mechanical anisotropy; Sheet metal.

---

<sup>1</sup> Corresponding author.

E–mail address: [m.karimi@shahroodut.ac.ir](mailto:m.karimi@shahroodut.ac.ir) (M. Karimi). Tel.: 98-9132894357

## 1. Introduction

Severe plastic deformation (SPD) processes are defined as the techniques that induce large plastic strains in materials, usually under high applied stresses and at relatively low temperatures (usually less than 0.4 of the melting temperature) [1, 2]. SPD processes are used for refining the grains of conventional bulk materials to produce submicron (100 nm–1.0  $\mu\text{m}$ ) or even nano (<100 nm) grained materials [3]. Since mechanical properties of polycrystalline materials considerably depend on the grain size, SPD processing is a potential candidate for producing materials with unusual and attractive mechanical properties [4].

A rather large body of research has been published on the role of different SPD techniques such as equal channel angular pressing (ECAP), high-pressure torsion (HPT) and accumulative roll bonding (ARB) on improvement of mechanical properties for a series of metallic materials [5–7]. Among various SPD techniques, the ARB process is widely used to manufacture ultra-fine grained sheets or plates since it utilizes a conventional rolling mill. The process consists of multiple cycles of surface preparation, stacking and roll bonding of material sheets [7].

In recent years, the ARB process has been used as an effective alternative method for manufacturing high-strength metal matrix composites (MMCs) [8]. In this method, reinforcements are added uniformly between the two strips after surface preparation and before stacking of sheets as shown schematically in Fig. 1. Generally, due to the combined effects of grain refinement and reinforcements, a significant increase of strength is achieved in the metals and MMCs produced by ARB [9, 10].

Although, ARB is a viable method for producing high strength metal sheets, many engineering applications require a combination of high ductility and strength. There are a few numbers of studies in which the ARB-processed materials are subjected to a second thermo-mechanical or heat treatment process to gain a good combination of strength and ductility [11, 12].

Despite extensive research works regarding the effect of ARB process on improving the mechanical properties of various metals, the majority of these studies have mainly focused on the mechanical properties of material in the rolling direction. Considering the nature of the ARB process in generating a large anisotropy of mechanical

properties, investigating the anisotropy of mechanical properties of materials produced by ARB process becomes a crucial topic [13].

It is known that mechanical anisotropy of deformed polycrystalline metals is controlled by factors such as crystallographic texture, orientation of precipitates, deformation microstructure and latent hardening [14, 15]. Latent hardening seems to be of less significance and is effective only up to small strains [14, 15], so that is not a source of anisotropy in severely deformed metals. Directionality of the deformed microstructure due to the presence of shear bands and dense dislocation walls can also influence mechanical anisotropy [15–18]. Moreover, some studies have demonstrated the importance of crystallographic texture [16, 19]. A strong texture developed by large plastic deformations and possible additional heat treatments processes may induce anisotropic behavior in the final product. In HCP metals, such as titanium, low symmetry of crystal structure and high critical resolved shear stress values of slip systems, leads to the restricted deformation of the material. This results in a complicated combination of slip and twinning systems to accommodate deformation in HCP metals [20, 21]. This complexity in deformation behavior of HCP metals may influence the texture and mechanical anisotropy of material.

Accordingly, the aim of present study was to evaluate the anisotropy of mechanical properties in commercial purity titanium (CP–Ti)/SiC composite sheets processed by ARB and subsequent annealing.

## **2. Experimental procedure**

### **2.1. Materials**

In this study, CP–Ti (ASTM grade 2) sheet, 1 mm in thickness, was used as the starting material. The sheet was cut into 200 mm × 50 mm strips, parallel to the sheet rolling direction. SiC powder with average particle size of 10 μm was used as reinforcement.

### **2.2. Accumulative roll bonding and annealing**

To prepare the surface before roll bonding, the strips were cleaned by acetone and roughened using a rotating wire cup brush having a wire diameter of 0.4 mm. After surface preparation, SiC particles were uniformly dispersed between the two strips,

followed by stacking over each other and then tightened to each other at both ends using steel wires. The volume percent of SiC particles was adjusted to 1.5%. The roll bonding process was carried out by 50% reduction in thickness (Von Mises equivalent strain of 0.8) with no lubrication at room temperature. The roll diameter and the roll peripheral speed were 220 mm and  $4.5 \text{ m}\cdot\text{min}^{-1}$ , respectively. The rolled specimen was cut into two halves, and the above-mentioned procedure was repeated up to eight cycles without adding any reinforcement particles (Fig. 1). This procedure resulted in a uniform distribution of particles as explained in our previous research work [8]. The material that undergoes two or more cycles of roll bonding process is called ARBed material. The 8 cycles ARBed sample was isothermally annealed at  $500 \text{ }^\circ\text{C}$  for 5 minutes in a muffle furnace. In our previous research work [12], these annealing conditions were introduced as optimal conditions for obtaining a good combination of strength and toughness.

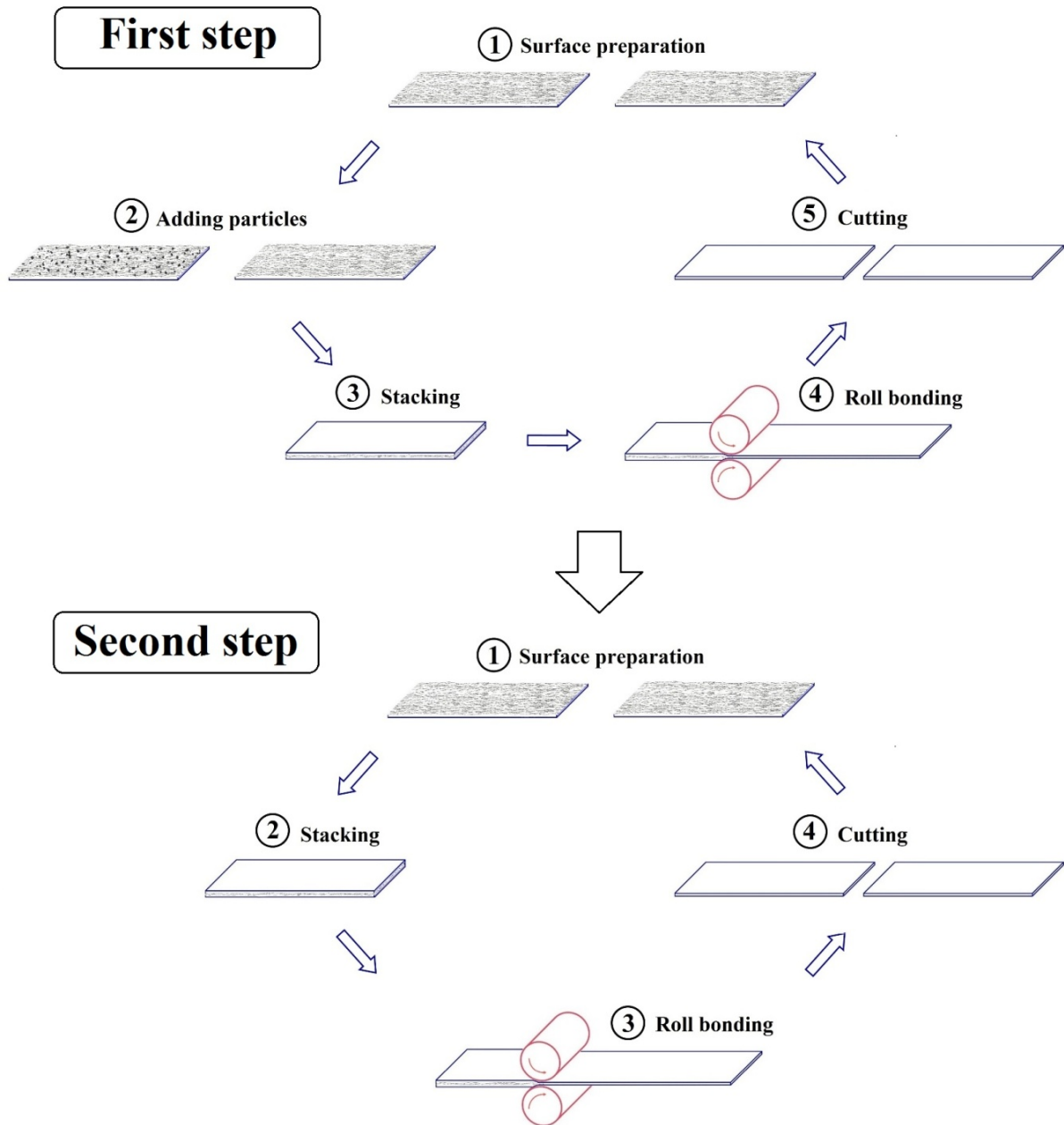


Fig. 1 Schematic illustration of producing composite by ARB process.

### 2.3. Mechanical properties

The specimens for tensile test were cut along planes coinciding with the rolling, diagonal (45 degrees to the rolling direction) and transverse directions (hereafter referred to as RD, DD and TD specimens, respectively). The specimens were wire cut to avoid burrs along the edge. The specimens having the gauge length of 25 mm and the gauge width of 4.8 mm were tested at room temperature by a Hounsfield–H50ks machine. The cross–head speed was 0.1 mm/min resulting in the initial strain rate of  $1.6 \times 10^{-3}/s$ .

The plastic strain ratio (Lankford value,  $r$ -value), an index of mechanical anisotropy of sheet metals in metal forming applications, was measured in three directions of RD ( $r_{RD}$ ), DD ( $r_{DD}$ ) and TD ( $r_{TD}$ ). The  $r$ -value is defined as the ratio of width strain to thickness strain and is expressed in the following form:

$$r = \frac{\ln \frac{w_0}{w}}{\ln \frac{b_0}{b}} \quad \text{equation (1)}$$

where  $w_0$  and  $b_0$  are the initial width and thickness of the gauge, respectively. Also,  $w$  and  $b$  are the width and the thickness of the gauge after deformation, respectively. As it is difficult to measure the strain in the thickness direction of a thin sheet accurately, it was calculated from the strains in the longitudinal and width directions using the volume constancy:

$$l_0 w_0 b_0 - l w b = 0 \quad \text{equation (2)}$$

$l_0$  and  $l$  are the initial gauge length in the tensile direction and that after deformation, respectively. Hence, the  $r$ -value can be calculated by equation 3:

$$r = \frac{\ln \frac{w_0}{w}}{\ln \frac{l w}{l_0 w_0}} \quad \text{equation (3)}$$

The average  $r$ -value ( $\langle r \rangle$ , a measure of normal anisotropy) and  $\Delta r$  (a measure of planar anisotropy) of the sheets are obtained from  $r_0$ ,  $r_{90}$  and  $r_{45}$ :

$$\langle r \rangle = \frac{1}{4}(r_{RD} + 2r_{DD} + r_{TD}) \quad \text{equation (4)}$$

$$\Delta r = \frac{1}{2}(r_{RD} - 2r_{DD} + r_{TD}) \quad \text{equation (5)}$$

The specimens were reloaded to measure the tensile strength and elongation.

#### 2.4. Texture measurements

To measure the texture of the sheets, X-ray diffraction (XRD) technique was used. Specimens (25 mm × 15 mm) were separated from different sheet samples. The texture of the specimens was measured on normal direction (ND) plane (RD–TD section) and in 0.25 mm under the surface of the specimens. These specimens were prepared by mechanical grinding and polishing. Texture was determined by measuring six incomplete pole figures (002), (100), (101), (102), (103), (110) using a general

area diffraction detector system (GADDS) attached to Bruker D8 Discover goniometer. Orientation distribution function (ODF) was constructed from six incomplete pole figures (PF), namely (002), (100), (101), (102), (103), (110). Recalculated pole figures were then plotted using the ODF.

### 3. Results and discussions

Fig. 2 shows  $\{0001\}$ ,  $\{10\bar{1}0\}$  and  $\{10\bar{1}1\}$  pole figures of CP-Ti sheet at different stages of process. It is noted from the pole figures that no strong crystallographic texture was developed for the starting Ti sheet.

Pole figures calculated for the sample ARBed by 2 cycles shows a TD split basal texture with basal poles tilted  $25^\circ$  away from the normal direction toward the transverse direction and the  $\langle 10\bar{1}0 \rangle$  poles aligned with the rolling direction (Fig. 2). Pole figures for the sample ARBed by 8 cycles also revealed preferred crystallographic orientation similar to that of 2 cycles ARBed sample, but with higher intensity. This texture is typical of cold-rolled HCP metals and alloys, possessing  $c/a$  ratio less than 1.633 [3].

Wang et al [3] found that during rolling of the metals and alloys, possessing  $c/a$  ratio less than 1.633 such as Zr (1.589) and Ti (1.587), textures with basal poles tilted  $\pm 20\text{--}40^\circ$  away from the normal direction toward the transverse direction is formed. Slip on prismatic planes is largely responsible for textures of these types.

The same texture was developed in the investigation of Chun et al. [22] during cold rolling of commercial-purity titanium. They conclude that for heavy deformation, between 60 and 90%, slip overrode twinning and shear bands developed. The crystal texture of deformed specimens was weakened by twinning but was strengthened by slip, resulting in a split-basal texture in heavily deformed specimens.

Development of this texture during ARB of CP-Ti is due to the fact that different HCP metals have different  $c/a$  ratio, leading to different deformation modes (slip and/or twinning). The  $c/a$  ratio determines the activation of the slip systems which in turn, affects the development of different crystallographic textures. The primary



deformation mode in Ti is the prismatic ( $\{10\bar{1}0\}\langle 11\bar{2}0\rangle$ ) slip, followed by pyramidal and basal ( $\{10\bar{1}1\}\langle 11\bar{2}0\rangle$  and  $\{0001\}\langle 11\bar{2}0\rangle$ ) slip systems. It has been found that slip on prismatic planes promotes spreading of basal pole during texture development [3].

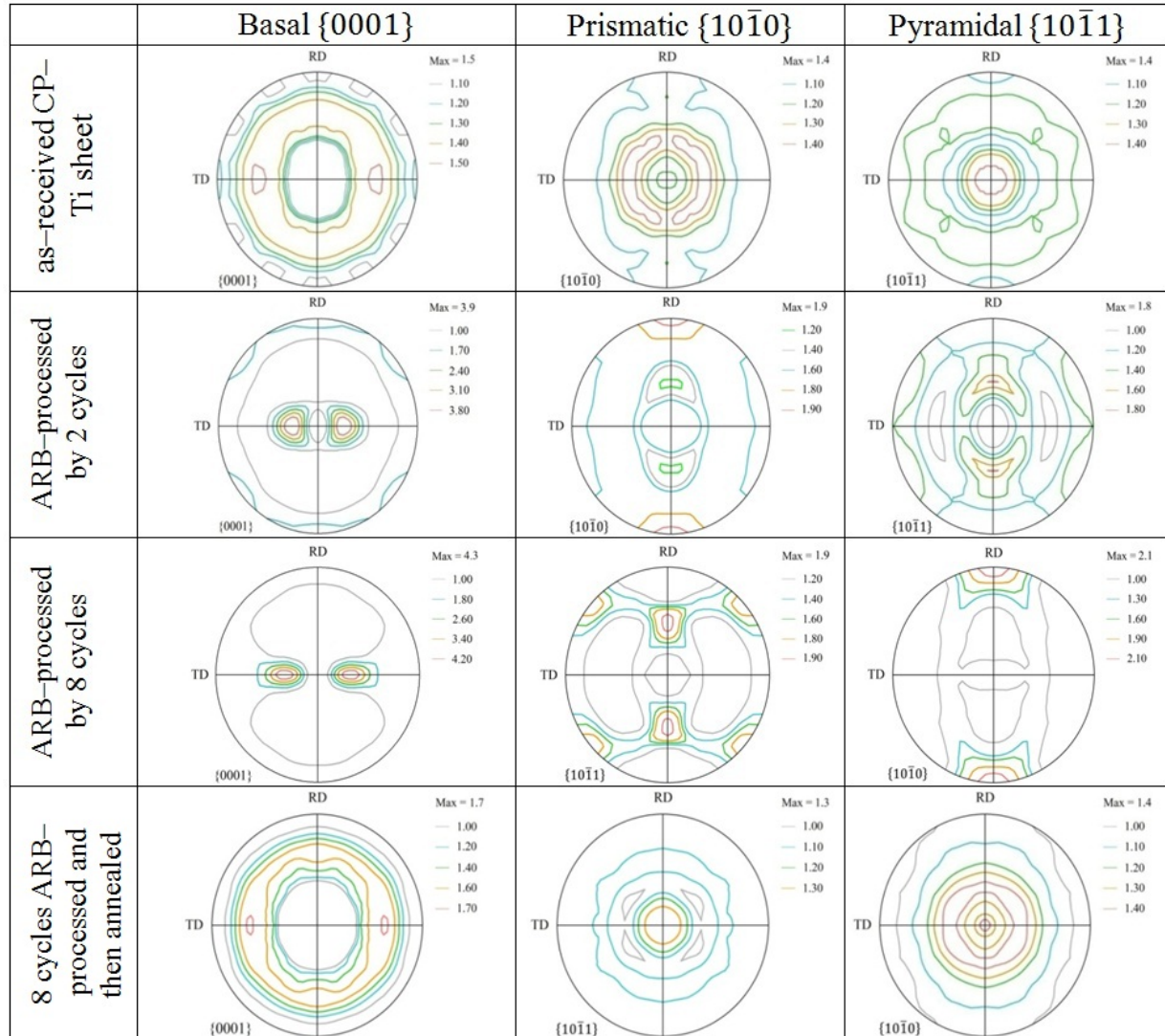


Fig. 2  $\{0001\}$ ,  $\{10\bar{1}0\}$  and  $\{10\bar{1}1\}$  pole figures obtained in normal direction of CP-Ti sheet at different stages of process.

Above mentioned crystallographic texture leads to the compaction of grains along the  $\langle 0001 \rangle$  directions, i.e. perpendicular to the basal plane located in the TD-ND plane. In such a case, most of  $\langle 10\bar{1}0 \rangle$  directions are arranged along the rolling direction, giving rise to the elongation of grains in this direction. It is also seen in Fig. 2 that after annealing, the intensity of ARB texture component decreased remarkably and almost no preferred orientation developed.

Fig. 3 displays the tensile test curves for different directions of starting titanium, ARBed and ARB–annealed sheets. As can be seen, the yield strength, tensile strength and elongation in RD, DD and TD specimens are almost identical, indicating isotropic mechanical behavior of the samples. Yield strength of the three samples was measured within the range of 268–290 MPa, tensile strength was in the range of 360–373 MPa and elongation was between 43.5 to 45.7%.

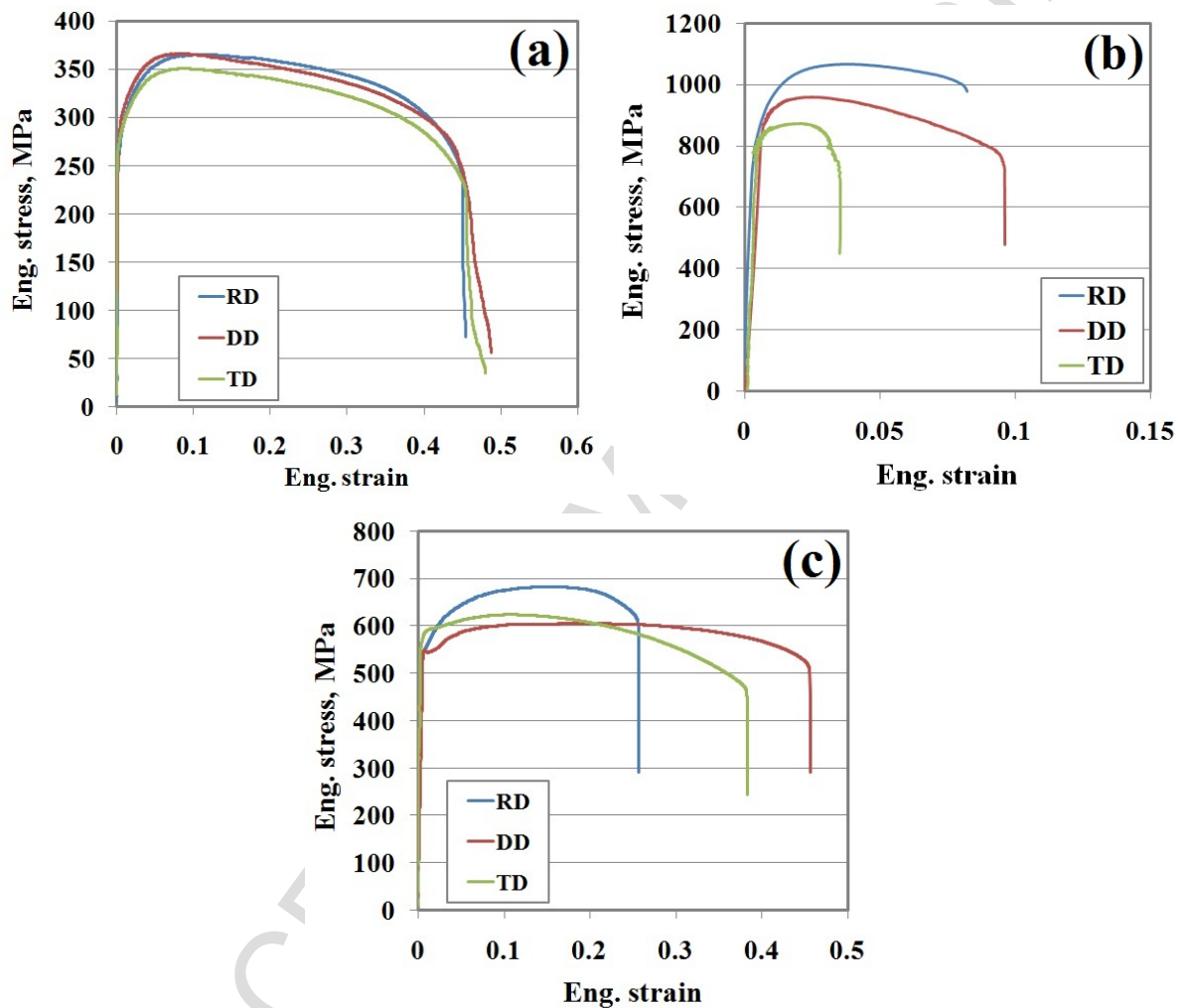


Fig. 3 Effect of tensile specimen orientation on the mechanical properties of (a) as-received CP-Ti sheet (starting titanium), (b) 8 cycles ARBed and (c) 8 cycles ARBed-subsequently annealed samples.

However, engineering stress–strain curves for the ARBed samples shows the high anisotropy of mechanical properties. This is shown for 8 cycles ARBed sample in Fig. 3b. Different stress–strain behavior is seen in TD compared to those of other

directions. Although, low uniform elongation is found for all three directions, RD and DD samples exhibited significantly higher necking elongation. It is also observed that the strength in the RD specimen is less than that for DD and TD specimens. Yield strength of the material in the rolling direction is measured 790 MPa and it is 785 and 765 MPa in the diagonal and transverse directions, respectively.

Fig. 3c displays engineering stress–strain curves for the 8 cycles ARBed–subsequently annealed sample. As can be seen, yield stress is not much different in three directions. However, similar to the ARBed samples, stress–strain behavior is not the same in three directions. By rotating from rolling towards the transverse direction of the sheet, the uniform elongation decreases.

Plastic anisotropy data for starting and ARB–annealed titanium are given in Table 1. ARB samples in this study shows very small uniform elongation (less than ~5%). Therefore, only the starting titanium and ARB–subsequently annealed samples are studied.

Table 1. Plastic anisotropy data for starting and ARB–annealed titanium

	Direction	Lankford Parameter (r–value)	Average r–value $\langle r \rangle = 1/4(r_0 + 2r_{45} + r_{90})$	Planar Anisotropy $\langle \Delta r \rangle = 1/2(r_0 - 2r_{45} + r_{90})$
Starting Titanium	RD	0.791	0.735	0.048
	DD	0.710		
	TD	0.726		
ARB and Annealed	RD	1.499	1.534	–0.434
	DD	1.751		
	TD	1.136		

In the starting titanium the r–value is almost identical for the three directions of testing. However, ARB–annealed sample shows its smallest r–value for TD. A low r–value corresponds to higher susceptibility of the sheet to thinning, meaning that ARB–annealed sheet has lower tendency for thinning in DD and RD specimens. This characteristic can be employed in deformation processes of the sheets such as deep drawing. For example, in a rectangular non–deformed sheet metal, if the TD is placed

along the middle of lateral sides and RD with higher  $r$ -value over the corners, superior results (i.e. larger drawing ratio and lower probability of thinning) are achieved.

Considering the fact that greater  $\langle r \rangle$  value results in lower susceptibility of the sheet to thinning, it can be concluded that the ARB-annealed sheet is more resistant to thinning compared to the starting titanium. On the other hand, the higher absolute  $\langle \Delta r \rangle$  value for ARB-annealed sheet represents higher anisotropy in the plane and consequently possible defects such as earing may form during deformation. Change in the sign of  $\langle \Delta r \rangle$  represents a shift in direction susceptible to thinning.

Higher resistance to thinning for the ARB-annealed sheet as compared to the starting titanium can be resulted from more uniform elongation in ARB-annealed state. The uniform elongation of the ARB-annealed sheets was 17.5, 20.5 and 12% for RD, DD and TD, respectively, while the uniform elongation of the starting titanium sheet was almost 10% for different directions.

Some researchers have shown that materials with very fine grain sizes (about one micrometer or less) usually have low uniform elongation [11, 23–25]. This is related to the high strength of ultrafine grained metals. Therefore, plastic instability occurs in the early stages of deformation during the tensile test. Condition for occurrence of plastic instability is expressed by the following criterion that represents the beginning of local deformation of the material:

$$\sigma \geq d\sigma/d\varepsilon \quad \text{equation (6)}$$

where  $\sigma$  is flow stress,  $\varepsilon$  is true strain and  $\frac{d\sigma}{d\varepsilon}$  is work hardening rate. This equation shows that the uniform elongation depends on the flow stress and work hardening rate of material. When the strength increases without remarkable increase in the work hardening rate, uniform elongation decreases. In many studies performed on the production of fine grain sizes (less than 2  $\mu\text{m}$ ), a reduction of the work hardening rate with grain refinement has been observed [11, 23–25]. However, some researchers did not provide justifications for such work-hardening behavior and some of them [25] related it to the reduced ability of dislocation accumulation with decreasing the grain size. On the other hand, it is well known that grain refinement increases strength, which in turn, reduces the uniform elongation.

The microstructure of starting titanium and ARB–annealed samples is shown in Fig. 4. A remarkable grain refinement can be seen after ARB and subsequent annealing. Additionally, initial coarse grained structure with a mean grain size of 54  $\mu\text{m}$  is transformed to an ultrafine grain recrystallized structure with a mean grain size of 1.45  $\mu\text{m}$ .

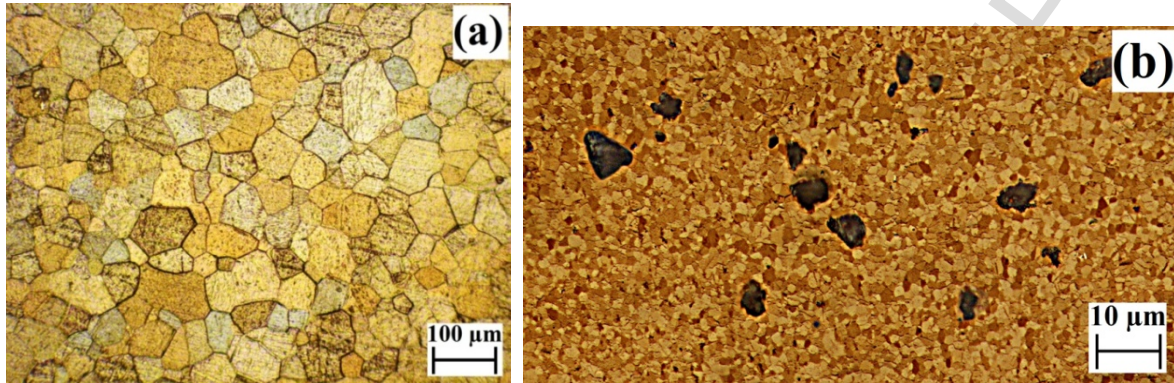


Fig. 4 Microstructure of (a) starting titanium and (b) ARB–annealed samples.

To discuss about the reason for increased uniform elongation of the ARB–annealed samples, a factor of normalized work hardening rate,  $\theta$ , can be defined as follows:

$$\theta = \frac{1}{\sigma} \left( \frac{d\sigma}{d\varepsilon} \right) \quad \text{equation (7)}$$

A material with a high amount of normalized work hardening rate usually has more uniform elongation.

Fig. 5 shows variations of the work hardening rate and normalized work hardening rate versus true plastic strain in the range of uniform elongation for the starting titanium and ARB–annealed RD samples. According to Fig. 5a, it is clear that in this investigation, due to the grain refinement after ARB and annealing process as well as adding the reinforcement particles, work hardening rate increases compared to the starting titanium specimen. The high work hardening rate of ARB–annealed material can be attributed to the short distance of dislocation movement before approaching to the obstacles, which are grain boundaries in this case. Small grain size also reduces the distance between dislocations leading to an increased resistance to deformation [26, 27]. In addition, the presence of particles can prevent the dynamic recovery and increase dislocation accumulation. Particles may act as barriers to dislocation motion,



which can give rise to increased work hardening. Fig. 5b shows that in the range of uniform plastic deformation, ARB–annealed sample, has slightly higher normalized work hardening rate. The conditions for occurrence of plastic instability (where normalized work hardening rate is equal to 1) are provided in larger strains, for ARB–annealed sample.

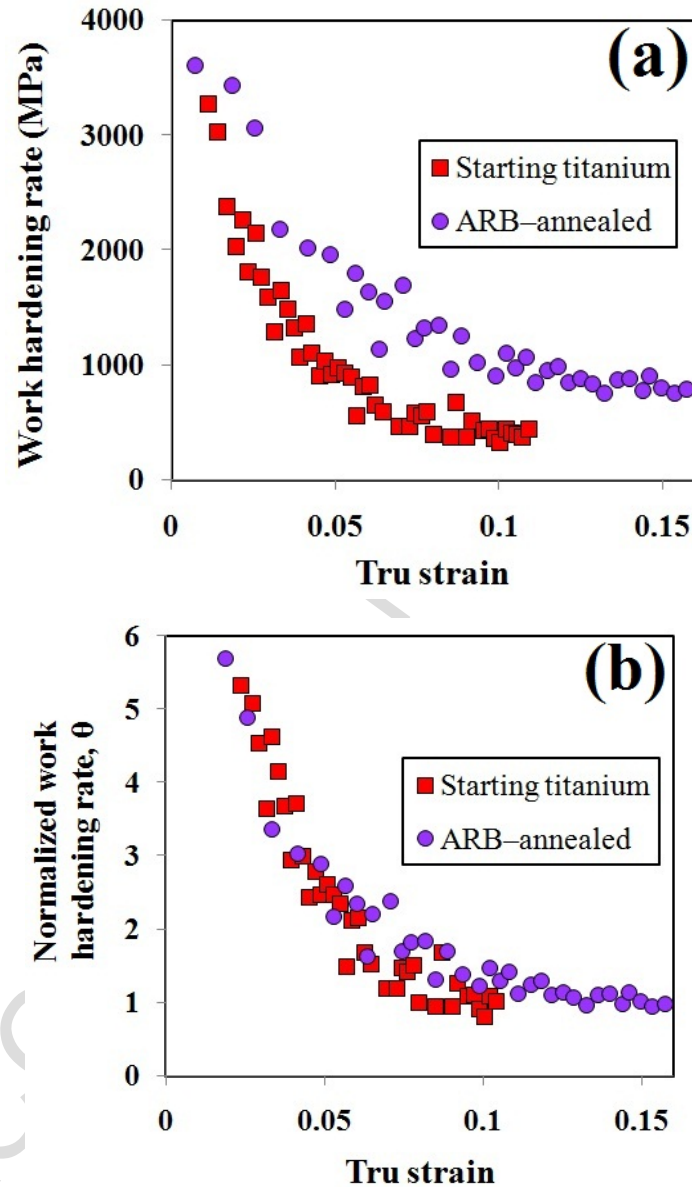


Fig. 5 Variations of (a) work hardening rate and (b) normalized work hardening rate versus true strain for starting titanium and ARB–annealed samples.

#### 4. Conclusion

Texture variations and plastic anisotropy for CP–Ti/SiC composite sheets subjected to ARB and subsequent annealing were evaluated. The main conclusions of this study can be summarized as follows:

- ARBed material showed a large anisotropy of mechanical properties in different directions. However, the anisotropy decreased after annealing.
- Based on measured  $r$ -values, it was determined that the ARB–annealed sheet has higher resistance to thinning during deformation, compared to the starting titanium. On the other hand, the higher absolute  $\langle \Delta r \rangle$  values for ARB–annealed sheet represented a higher anisotropy in the plane, which in turn, increases the possible formation of defects, i.e. earing, during deformation.
- Higher resistance to thinning of the ARB–annealed sheet compared to the starting titanium was attributed to its higher uniform elongation. Furthermore, remarkable uniform elongation of ARB–annealed sample was ascribed to higher work hardening rate, which was a direct result of fine grain size.

#### References

- [1] L.S. Toth, C. Gu, *Mater. Charact.* 2014, vol. 92, pp. 1–14.
- [2] R.Z. Valiev, R.K. Islamgaliev, I.V. Alexandrov, *Prog. Mater. Sci.* 2000, vol. 45, pp. 103–189.
- [3] R.B. Figueiredo, T.G. Langdon, *J. Mater. Res. Tech.*, 2012, vol. 1, pp. 55–62.
- [4] A. Azushima, R. Kopp, A. Korhonen, D.Y. Yang, F. Micari, G.D. Lahoti, P. Groche, J. Yanagimoto, N. Tsuji, A. Rosochowski, A. Yanagida, *CIRP Annals–Manuf. Tech.*, 2008, vol. 57, pp. 716–735.
- [5] Y. Zhang, R.B. Figueiredo, S.N. Alhajeri, J.T. Wang, N. Gao, T.G. Langdon, *Mater. Sci. Eng. A*, 2011, vol. 528, pp. 7708–7714.
- [6] A.A. Popov, I.Y. Pyshmintsev, S.L. Demakov, A.G. Illarionov, T.C. Lowe, A.V. Sergeyeva, R.Z. Valiev, *Scripta Mater.*, 1997, vol. 37, pp. 1089–1094.
- [7] D. Terada, S. Inoue, N. Tsuji, *J. Mater. Sci.*, 2007, vol. 42, pp. 1673–1681.
- [8] M. Karimi, M.R. Toroghinejad, *Mater. Des.*, 2014, vol. 59, pp. 494–501.

- [9] R. Jamaati, M.R. Toroghinejad, *Mater. Sci. Eng. A*, 2010, vol. 527, pp. 7430–7435.
- [10] R. Jamaati, M.R. Toroghinejad, S. Amirkhanlou, H. Edris, *Mater. Sci. Eng. A*, 2015, vol. 639, pp. 656–662.
- [11] D. Terada, M. Inoue, H. Kitahara, N. Tsuji, *Mater. Trans.*, 2008, vol. 49, pp. 41–46.
- [12] M. Karimi, M.R. Toroghinejad, Kh. Farmanesh, *Mater. Des.*, 2015, vol. 65, pp. 34–41.
- [13] B. Beausir, J. Scharnweber, J. Jaschinski, H.G. Brokmeier, C.G. Oertel, W. Skrotzki, *Mater. Sci. Eng. A*, 2010, vol. 527, pp. 3271–3278.
- [14] D.J. Jensen, N. Hansen, *Acta Metall. Mater.*, 1990, vol. 38, pp. 1369–1380.
- [15] N. Hansen, D.J. Jensen, *Acta Metall. Mater.*, 1992, vol. 40, pp. 3265–3275.
- [16] G. Winther, D.J. Jensen, N. Hansen, *Acta Mater.*, 1997, vol. 45, pp. 2455–2465.
- [17] N. Hansen, H. Xiaoxu, *Mater. Sci. Eng. A*, 1997, vol. 234, pp. 602–605.
- [18] Z.J. Li, G. Winther, N. Hansen, *Mater. Sci. Eng. A*, 2004, vol. 387, pp. 199–202.
- [19] P.H. Lequeu, J.J. Jonas, *Metall. Trans. A*, 1988, vol. 19, pp. 105–120.
- [20] Y.N. Wang, J.C. Huang, *Mate. Chem. Phys.*, 2003, vol. 81, pp. 11–26.
- [21] M. Karimi, M.R. Toroghinejad, J. Dutkiewicz, *Mater. Character.*, 2016, vol. 122, pp. 98–103.
- [22] Y.B. Chun, S.H. Yu, S.L. Semiatin, S.K. Hwang, *Mater. Sci. Eng. A*, 2005, vol. 398, pp. 209–219.
- [23] L. Ghalandari, M.M. Moshksar, *J. Alloy. Comp.*, 2010, vol. 506, pp. 172–178.
- [24] K.X. Wei, W. Wei, Q.B. Du, J. Hu, *Mater. Sci. Eng. A*, 2009, vol. 525, pp. 55–59.
- [25] Y.H. Zhao, X.Zh. Liao, Sh. Cheng, E. Ma, Y.T. Zhu, *Adv. Mater.*, 2006, vol. 18, pp. 2280–2283.
- [26] A.Z. Mohamed, M.M. Mostafa, M.S. Sakr, A.A. El-Daly, *Phys. Status Solidi A*, 1988, vol. 110, pp. 13–17.
- [27] Ch. Kwan, Zh. Wang, S.B. Kang, *Mater. Sci. Eng. A*, 2008, vol. 480, pp. 148–159.



**Figure captions**

Fig. 1 Schematic illustration of producing composite by ARB process.

Fig. 2  $\{0001\}$ ,  $\{10\bar{1}0\}$  and  $\{10\bar{1}1\}$  pole figures obtained in normal direction of CP-Ti sheet at different stages of process.

Fig. 3 Effect of tensile specimen orientation on the mechanical properties of (a) as-received CP-Ti sheet (starting titanium), (b) 8 cycles ARBed and (c) 8 cycles ARBed-subsequently annealed samples.

Fig. 4 Microstructure of (a) starting titanium and (b) ARB-annealed samples.

Fig. 5 Variations of (a) work hardening rate and (b) normalized work hardening rate versus true strain for starting titanium and ARB-annealed samples.

**Table caption**

Table 1. Plastic anisotropy data for starting and ARB-annealed titanium

ACCEPTED MANUSCRIPT

- Titanium/SiC composite was produced by ARB and subsequent annealing.
- Texture evolution and plastic anisotropy of a material were studied.
- ARBed sample showed a large anisotropy of mechanical properties and strong texture.
- ARB–annealed sheet exhibited relatively low susceptibility to thinning.
- ARB–annealed sheet had more planar anisotropy compared with the raw titanium.